JOURNAL OF THERMOPHYSICS AND HEAT TRANSFER
Vol. 9, No. 3, July–September 1995

Vibrational Nonequilibrium Modeling Using Direct Simulation Part 1: Continuous Internal Energy

Isabelle Choquet*
ONERA, 92322 Châtillon, France

A new class of vibrational nonequilibrium models is introduced for repulsive–attractive intermolecular potentials to reproduce on average the relaxation time of Millikan and White over all its domain of validity. Intended to do Monte Carlo simulations, it is proposed at a microscopic scale, in the form of individual probabilities of vibration translation energy exchange p. In this first part the internal energy is assumed to be continuous. The relation linking the required individual probability to the relaxation time to be reproduced is solved thanks to the systematic and exact resolution method, based on the Laplace transformation, that we had proposed earlier. Models previously introduced by Boyd and Bird are found as borderline cases of the present one. Attainment of detailed balance is checked with homogeneous calculations, using the direct simulation Monte Carlo method and the original Borgnakke–Larsen (BL) scheme. Assumption used to develop p models is discussed in light of numerical results and justified thanks to a recent mathematical study of the BL scheme.

I. Introduction

THERMAL nonequilibria of vibration appear in various kinds of flows characterized by a high enthalpy. As a direct consequence, they modify temperature distributions in the flowfield. Moreover, they have significant secondary effects since they can affect heat fluxes, and also chemical reaction rates due to the strong coupling between vibration and chemistry. Taking them into account is thus a necessary stage to model high enthalpy flows.

Concerning specifically rarefied gases, flows in thermal nonequilibria are generally simulated numerically using the direct simulation Monte Carlo (DSMC) method introduced by Bird[1] and the numerical scheme proposed by Borgnakke and Larsen[2] for inelastic collisions. This corresponds to a probabilistic description of the flow at a microscopic scale, considering sets of particles. The first model of vibrational nonequilibrium,[2] was associated with a constant inelastic collision number. Since it does not reproduce the temperature dependence of relaxation times experimentally observed, the challenge is, until then, to develop models reproducing on average a relaxation time correlated with experimental results. One can distinguish two approaches: 1) macroscopic and 2) microscopic. The former uses directly relaxation times, such as Millikan and White data[3] τ_v^{MW}. In this way, both relaxation time and detailed balance are satisfied numerically. But, in a computational point of view, time penalty is significant since temperature must be determined in each cell and at each time step. We opt for the second approach. It requires the knowledge of individual probabilities of energy exchange p. It avoids time penalty, but raises other difficulties. One can refer to pioneering models proposed by Boyd[4,5] intending to reproduce on average τ_v^{MW}. They are associated with repulsive intermolecular potentials through the collision cross section of variable hard sphere[6] (VHS). They have been approximated thanks to the steepest descent method and expressed as functions of the relative velocity norm. They raised two problems:

1) The resolution method implies a significant reduction of p domain of validity in comparison with the τ_v^{MW} domain of validity. Indeed, the temperature is supposed to be smaller than the characteristic temperature of vibrational excitation.

2) Homogeneous calculations made using the DSMC method and the original Borgnakke–Larsen (BL) scheme do not reproduce detailed balance at equilibrium (see below).

Next, as Boyd did for rotation,[7] Bird[8] proposed individual probabilities of vibration depending on the total energy involved in the collision, instead of the relative velocity norm. His empirical model always satisfied the second point, that is detailed balance at equilibrium. However, it overestimates the time needed to reach equilibrium (cf. below). Concurrently, collisional models have been improved. One can refer to the variable soft sphere model introduced by Koura and Matsumoto[9] or the generalized hard sphere (GHS) model proposed by Hash and Hassan.[10]

This article's purpose is to propose a new class of models for vibration translation energy exchange, assuming in this first part a continuous internal energy. Contrary to studies previously mentioned,[4] we do not introduce temperature limitation to preserve the domain of validity of τ_v^{MW}. Moreover, individual probabilities are developed within a larger frame than the previous ones.[4,8] They are associated not only with repulsive, but also with attractive–repulsive intermolecular potentials through the GHS collision cross section.[10] They are derived to reproduce on average the vibrational relaxation time of Millikan and White. For this purpose, the problem formulation and the new resolution method introduced in Ref. 11 are briefly recalled. On a first assumption we expressed p as a function of the relative velocity norm, to check whether problems of detailed balance that have been observed with Boyd's model are due, or not, to the approximated resolution method. The exact p family, introduced later, includes as a borderline case the vibrational model proposed by Boyd.[4] It is then shown that neither exact or approximated p reproduces numerically the equipartition of energy at equilibrium within the frame of the original BL scheme. This point, already discussed for rotational nonequilibria[11] in light of a recent mathematical study,[12] is justified. In order to verify detailed balance at equilibrium, another assumption, used by Bird, is investigated and a justification is also proposed. The individual probability is expressed as a function of the total energy involved in the exchange. Again, the class of p models derived hereafter includes, as a borderline case, the empirical model of vibration proposed by Bird.[8] Both model classes are stated (Sec. III), in a global expression. Key points of the demonstration are detailed in Sec. IV. These p models are validated

Received April 28, 1994; revision received Oct. 18, 1994; accepted for publication Nov. 8, 1994.

*Research Scientist; currently at Laboratoire d'Aérothermique, CNRS, 4 ter route des Gardes, 92190 Meudon, France.

in Sec. V, using the DSMC method and the original BL scheme. Calculations are carried out to check if the equilibrium state is well-reproduced at the macroscopic scale. They are realized considering the homogeneous unsteady problem of a pure diatomic gas of nitrogen, initially presenting a nonequilibrium between vibrational and translational modes. According to the numerical results obtained, the variable used to determine p is discussed and justified.

II. Problem Formulation

A system of two particles, $P1$ and $P2$, is considered. They are characterized by ζ_t translational degrees of freedom (DOFs), $\zeta_{1,v}$ and $\zeta_{2,v}$ DOFs of vibration, and internal energies of vibration $e_{1,v}$ and $e_{2,v}$. The collisional system, $P1 - P2$, is characterized by the reduced mass μ, the relative velocity norm g, the vibrational DOFs $\zeta_v = \zeta_{1,v} + \zeta_{2,v}$, and the vibrational energy $e_v = e_{1,v} + e_{2,v}$. The total energy involved in the exchange under consideration is denoted by $e = (\mu g^2)/2 + e_v$.

The problem formulation consists in linking the required individual probability of vibration translation energy exchange p, to the average probability $\langle p \rangle$ (depending on the relaxation time to be reproduced). The problem is stated in Ref. 11 for any total collision cross section $\sigma_T(g)$. It is established starting from the Boltzmann equation and setting the assumptions required to obtain a well-stated problem. Besides obvious hypothesis (cf. Ref. 11, $H1$ to $H3$), one assumes that, $H4$: the individual probability of energy exchange depends only on one variable, $H4a$: the total energy involved in the exchange e, or $H4b$: the relative velocity norm g.

The next and last hypothesis is new. It is due to the rigorous mathematical study of the original BL scheme,[2] carried out by Bourgat et al.[12] for a continuous internal energy. This assumption brings a necessary and sufficient condition for the entropy theorem to be satisfied.

$H5$: in the case of inelastic collisions, if σ_T and p depend on the relative velocity norm and not on a collisional invariant, they must be homogeneous with respect to the g variable

$$\forall\, r \in \mathbb{R}, \qquad \exists\, \nu_0 \in \mathbb{R} \,/\, \sigma_T(rg)p(rg) = r^{\nu_0}\sigma_T(g)p(g) \tag{1}$$

If $H5$ is not respected, then the entropy theorem is violated. Consequently, the equipartition of energy is generally not verified at equilibrium. This point is illustrated later in Sec. V.

The problem[11] is recalled here considering the GHS collisional model[10] introduced for attractive–repulsive intermolecular potentials

$$\sigma_T(g) = \sum_{j=1}^{jmax} \kappa_j g^{-2\omega_j} \tag{2}$$

where κ_j and ω_j are constants. In the particular case $jmax = 1$, relation (2) reduces to the VHS model, used until then to model vibrational nonequilibrium. A new resolution method of the problem under consideration has also been proposed in Ref. 11. It has been pointed out doing the change of variables

$$y_i = \phi_i^{\gamma_i}, \qquad \varepsilon_i = h_i T^{-1} \tag{3}$$

with $i = 1$ or 2 and

$$\phi_1 = e, \qquad \phi_2 = g \tag{4a}$$

$$h_1 = 1/k, \qquad h_2 = \mu/(2k) \tag{4b}$$

where k is Boltzmann's constant and T is the equilibrium temperature. Then, the derivation of p reduces to the determination of the inverse Laplace transform $\xi = L^{-1}[\Xi]$ of the Ξ function,[11] such as

$$\xi[y_i] = p[y_i^{1/\gamma_i}] \sum_{j=1}^{jmax} \kappa_{i,j} \frac{\Gamma[\gamma_2 - \omega_j]}{\Gamma[\gamma_i - \omega_j]} y_i^{\gamma_i - \omega_j - 1} \tag{5a}$$

$$\Xi[\varepsilon_i] = \langle p \rangle [h_i \varepsilon_i^{-1}] \sum_{j=1}^{jmax} \kappa_{i,j} \Gamma[\gamma_2 - \omega_j] \varepsilon_i^{-\gamma_i + \omega_j} \tag{5b}$$

with

$$\gamma_2 = \zeta_t/2 + 1/2, \qquad \gamma_1 = \gamma_2 + \zeta_v/2, \qquad \kappa_{i,j} = \kappa_i (h_2 h_i^{-1})^{\omega_j - 1/2} \tag{6}$$

where Γ is the mathematical function and $\langle p \rangle$ the average probability; it depends on the relaxation time to be reproduced and is detailed later in this article.

Let us recall that the previous resolution method of the problem was not based on the Laplace transformation. The required p was postulated by making use of parameters. Then, it was averaged in an exact way,[7] or an approximate one,[4,5,8] according to the problem difficulty. Finally, parameters were obtained by identification in simple cases and, otherwise, by fitting. In the latter case, the p domain of validity could be significantly decreased. For instance, one can refer to vibrational nonequilibrium models,[4] developed using the steepest descent method and evoked in Sec. I.

Using our original procedure, based on the Laplace transformation, we start from a given average probability (correlated with experimental results) to determine, in a systematic and exact way, an analytical (or numerical) expression of p. Contrary to the procedure used until then, it allows bypassing both restrictive derivation hypothesis and a determination a priori of the required p. In this way, it makes feasible the development of p models reproducing on average all the domain of validity of the Millikan and White relaxation time. Furthermore, it allows extending these p models of vibration translation energy exchange to repulsive–attractive intermolecular potentials.

III. Problem Resolution: Data and Results

Referring to the study carried out by Haas et al.[13] and extended to the GHS cross section by Hash et al.,[14] the average probability of energy exchange expresses $\Lambda_{t,v}/(\langle \nu_c \rangle \tau_v)$ where

$$\Lambda_{t,v} = 1 + \frac{\zeta_v}{2} \left\{ \sum_{j=1}^{jmax} \kappa_j \Gamma[\gamma_2 - \omega_j] \varepsilon_2^{\omega_j} \right\} \times \left\{ \sum_{j=1}^{jmax} \kappa_j \Gamma[\gamma_2 + 1 - \omega_j] \varepsilon_2^{\omega_j} \right\}^{-1} \tag{7}$$

The vibrational relaxation time of Millikan and White[3] has been obtained by correlation between the theoretical model of Landau and Teller[15] and experimental results. It is given by

$$\tau_v = \tau_v^{MW} = (1/\rho k T) \exp(A T^{-1/3} + B) \tag{8}$$

where ρ is the number density, T the equilibrium temperature, and A and B are constants characteristic of the chemical species. The average collision frequency[11] associated with the GHS model[10] writes

$$\langle \nu_c \rangle = \alpha_t \rho \pi^{\zeta_t/2} \sum_{j=1}^{jmax} \kappa_j \Gamma[\gamma_2 - \omega_j] (h_2 T^{-1})^{\omega_j - 1/2} \tag{9}$$

where α_t depends only on ζ_t, and is defined[11] by $d\|\boldsymbol{g}\| = \alpha_t g^{\zeta_t - 2}\, dg^2$.

If the temperature dependence of Λ_{Ci}, which is very weak, is neglected, the derivation detailed in the next section leads to the analytical expression below, associated with the GHS collisional model, with a continuous internal energy and reproducing on average the vibrational relaxation time of Millikan and White

$$p(y_i^{1/i}) = \xi(y_i)\left\{\sum_{j=1}^{jmax} \kappa_{i,j}\frac{\Gamma[\gamma_2 - \omega_j]}{\Gamma[\gamma_i - \omega_j]}\, y_i^{\gamma_i-\omega_j-1}\right\}^{-1} \tag{10a}$$

$$\xi(y_i) = \alpha\Lambda\left\{\sum_{j=2E(\eta_i)+3}^{2E(\eta_i)+3} c_j(\nu, y_i^*)K_{\nu+j}[y_i^*] + \pi 3^{1/2}c(\nu, y_i^*)\int_{y_i}^{\infty} Ai[x]\,dx\right\} \tag{10b}$$

with

$$\alpha = \frac{\Lambda_{Ci}kh_i\pi^{\zeta_i/2}}{\alpha_i}\exp[-B] \tag{11a}$$

$$\beta = Ah_i^{1/3} \tag{11b}$$

$$\eta_i = \tfrac{1}{2} + \gamma_i \tag{11c}$$

$$\lambda = 2\left(\frac{\beta}{3}\right)^{3/2} \tag{11d}$$

$$y_i^* = \lambda y_i^{1/2} = \lambda\phi_i^{i/2} \tag{11e}$$

$$\Lambda = \frac{3^{1/2}}{\pi\Gamma[E(\eta_i) - 2D(\eta_i)]}\lambda^{2E(\eta_i)+2}\left(\frac{\beta}{3}\right)^{3D(\eta_i)} \tag{11f}$$

$$y_i^{**} = (3/2y_i^*)^{2/3} \tag{11g}$$

where $E(\eta_i)$ is the integer part of η_i and $D(\eta_i)$ is its decimal part. K_ν is the Hankel function of the second kind of parameter ν and Ai the airy function. The coefficients $c_j(\nu, y_i^*)$ and $c(\nu, y_i^*)$ are given explicitly in the Appendix. The individual probability p is calculated thanks to the tabulations of the K_ν and Ai functions, provided within the range]0; 9] by the mathematical library NAG for instance. This range is not sufficient to cover the domain of relative velocity norm or of total energy in which we are interested. The asymptotic expansion of p [Eq. (10a)] is required when y_i is in the vicinity of zero. Then, the ξ function defined in Eq. (10b) reduces to the following alternate series:

$$\xi(y_i) = \alpha\Lambda\left(\frac{\pi}{2}\right)^{1/2} y_i^{1/2}\exp(-y_i^*)\sum_{j=0}^{\infty} d_j(y_i^*)^j \tag{12}$$

Coefficients d_j are given in Tables 1 and 2. This asymptotic expansion is developed up to the 25th order to obtain a good fit between Eqs. (10b) and (12) in the vicinity of zero.

As expected, when *jmax* is set to unity, the individual probability associated with the VHS collisional model is recovered.[16] In the particular case of three DOFs in the velocity space, i.e., $\zeta_t = 3$, if 1) Λ_{Ci} is set to unity, 2) ϕ_i represents the relative velocity norm, 3) only one term of the GHS model is considered (that is to say for a VHS collisional model), and 4) only the first nonzero term of the asymptotic expansion valid in the vicinity of zero is taken into account, then the expression derived by Boyd,[4] thanks to the steepest descent method, is recovered.

In the same way, when ϕ_i represents the total energy involved in the exchange, the model introduced by Bird[8] is recovered as a borderline case.

Notice that, to consider the temperature dependence of Λ_{Ci}, the exact derivation of ξ (and thus p) can be carried out numerically.

Table 1 Coefficients d_j

j	$\zeta_t = 3, i = 2$	$\zeta_t = 3, i = 1$ $\zeta_{1,v} = 2, \zeta_{2,v} = 0$	$\zeta_t = 3, i = 1$ $\zeta_{1,v} = \zeta_{2,v} = 2$
0	0	0	0
1	0	0	0
2	1	0	0
3	-2.56944×10^{0}	0	0
4	$+9.03019 \times 10^{0}$	0	0
5	-4.06738×10^{1}	2	0
6	$+2.23764 \times 10^{2}$	-1.61339×10^{1}	0
7	-1.45458×10^{3}	$+1.22963 \times 10^{2}$	0
8	$+1.09096 \times 10^{4}$	-1.00357×10^{3}	8
9	-9.27329×10^{4}	$+8.97788 \times 10^{3}$	-1.32556×10^{2}
10	$+8.80965 \times 10^{5}$	-8.81991×10^{4}	$+1.75113 \times 10^{3}$
11	-9.25015×10^{6}	$+9.47909 \times 10^{5}$	-2.24011×10^{4}
12	$+1.06377 \times 10^{8}$	-1.10864×10^{7}	$+2.93525 \times 10^{5}$
13	-1.32971×10^{9}	$+1.40342 \times 10^{8}$	-4.02186×10^{6}
14	$+1.79512 \times 10^{10}$	-1.91313×10^{9}	$+5.80866 \times 10^{7}$
15	-2.60291×10^{11}	$+2.79530 \times 10^{10}$	-8.86603×10^{8}
16	$+4.03451 \times 10^{12}$	-4.35931×10^{11}	$+1.43037 \times 10^{10}$
17	-6.65694×10^{13}	$+7.22876 \times 10^{12}$	-2.43664×10^{11}
18	$+1.16496 \times 10^{15}$	-1.27024×10^{14}	$+4.37593 \times 10^{12}$
19	-2.15518×10^{16}	$+2.35801 \times 10^{15}$	-8.26984×10^{13}
20	$+4.20261 \times 10^{17}$	-4.61144×10^{16}	$+1.64153 \times 10^{15}$
21	-8.61534×10^{18}	$+9.47674 \times 10^{17}$	-3.41595×10^{16}
22	$+1.85230 \times 10^{20}$	-2.04181×10^{19}	$+7.43862 \times 10^{17}$
23	-4.16767×10^{21}	$+4.60248 \times 10^{20}$	-1.69213×10^{19}
24	$+9.79403 \times 10^{22}$	-1.08330×10^{22}	$+4.01442 \times 10^{20}$

Table 2 Coefficients d_j

j	$\zeta_t = 3, i = 2$	$\zeta_t = 2, i = 1$ $\zeta_{1,v} = 2, \zeta_{2,v} = 0$	$\zeta_t = 2, i = 1$ $\zeta_{1,v} = \zeta_{2,v} = 2$
0	0	0	0
1	0	0	0
2	0	0	0
3	$+2.00000 \times 10^{0}$	0	0
4	-8.13889×10^{0}	0	0
5	$+3.84076 \times 10^{1}$	0	0
6	-2.15774×10^{2}	8	0
7	$+1.41851 \times 10^{3}$	-8.45556×10^{1}	0
8	$+1.07110 \times 10^{4}$	$+7.87797 \times 10^{2}$	0
9	$+9.14406 \times 10^{4}$	-7.55937×10^{3}	$+4.80000 \times 10^{1}$
10	-8.71271×10^{5}	$+7.74881 \times 10^{4}$	-9.63333×10^{2}
11	$+9.16773 \times 10^{6}$	-8.56469×10^{5}	$+1.48418 \times 10^{4}$
12	-1.05594×10^{8}	$+1.02151 \times 10^{7}$	-2.16037×10^{5}
13	$+1.32149 \times 10^{9}$	-1.31174×10^{8}	$+3.16539 \times 10^{6}$
14	-1.78565×10^{10}	$+1.80753 \times 10^{9}$	-4.78715×10^{7}
15	$+2.59109 \times 10^{11}$	-2.66316×10^{10}	$+7.55428 \times 10^{8}$
16	-4.01855×10^{12}	$+4.18075 \times 10^{11}$	-1.24962×10^{10}
17	$+6.63380 \times 10^{13}$	-6.96966×10^{12}	$+2.17032 \times 10^{11}$
18	-1.16138×10^{15}	$+1.23005 \times 10^{14}$	-3.95785×10^{12}
19	$+2.14927 \times 10^{16}$	-2.29167×10^{15}	$+7.57288 \times 10^{13}$
20	-4.19225×10^{17}	$+4.49530 \times 10^{16}$	-1.51853×10^{15}
21	$+8.59619 \times 10^{18}$	-9.26182×10^{17}	$+3.18679 \times 10^{16}$
22	-1.84856×10^{20}	$+1.99989 \times 10^{19}$	-6.98909×10^{17}
23	$+4.16001 \times 10^{21}$	-4.51652×10^{20}	$+1.59952 \times 10^{19}$
24	-9.77757×10^{22}	$+1.06482 \times 10^{22}$	-3.81444×10^{20}

IV. Problem Resolution: Demonstration

The relation (10a), associated with a continuous internal energy, is derived from the inverse Laplace transform ξ of the Ξ function [Eq. (5b)], when considering the average collision frequency of the GHS model [Eq. (9)], and the vibrational relaxation time of Millikan and White [Eq. (8)]

$$\xi(y_i) = L^{-1}\left\{\langle p\rangle[h_i\varepsilon_i^{-1}]\sum_{j=1}^{jmax}\kappa_{i,j}\Gamma[\gamma_2 - \omega_j]\varepsilon_i^{\gamma_i+\omega_j}\right\} \tag{13a}$$

with

$$\langle p\rangle[h_i\varepsilon_i^{-1}] = \frac{\Lambda_{ci}}{\langle\nu_c\rangle\tau_c} = \frac{\Lambda_{ci}kh_i\varepsilon_i^{-1}\exp[-Ah_i^{-1/3}\varepsilon_i^{1/3} - B]}{\alpha_i\pi^{\zeta_i/2}\sum_{j=1}^{jmax}\kappa_{i,j}\Gamma[\gamma_2 - \omega_j]\varepsilon_i^{\omega_j-1/2}} \tag{13b}$$

α and β are introduced in Eqs. (11a) and (11b), respectively, in order to reduce the notations. Relation (13a) reads

$$\xi[y_i] = L^{-1}\{\alpha\varepsilon_i^{1/2-\gamma_i}\exp[-\beta\varepsilon_i^{1/3}]\} \tag{14}$$

When *jmax* is set to unity (VHS cross section), Λ_{ci} is a constant characteristic of the chemical species. Otherwise, (*jmax* > 1), the weak temperature dependence of Λ_{ci} is neglected to derive rapidly an analytical expression of p. Therefore, α is a constant, characteristic of the chemical species under consideration. Then, thanks to properties of Laplace transforms,[17] Eq. (14) yields

$$\xi[y_i] = \alpha\varphi[y_i] \tag{15a}$$

with

$$\varphi[y_i] = L^{-1}\{\varepsilon_i^{-\eta_i}\exp[-\beta\varepsilon_i^{1/3}]\} \tag{15b}$$

where η_i is defined in Eq. (11c). $\varphi[y_i]$ is then obtained carrying out the following steps:

*S*1: first, showing that this inverse Laplace transform φ, which expression is not directly known, can be replaced by an integral of the Hankel function of the second kind and of parameter $\nu = \frac{1}{3}$.

*S*2: next, the integral is expressed with the help of Hankel functions of the second kind and the Airy function.

A. Step *S*1: Integral

The main difficulty met with φ derivation comes from the exponential term. Various approaches can be taken up. At first, the exponential had been replaced by its series expansion. But this approach was abandoned since the individual probability obtained leads to problems of numerical convergence. Thus, the φ function has been expressed in a different way in order to avoid the problem of numerical estimation. In that aim, the exponential has been handled separately and directly, thanks to the relations[17]

$$L^{-1}\{\varepsilon^{-3/2}\exp[-3\varepsilon^{1/3}]\} = \frac{3^{1/2}}{\pi y^{1/2}}K_{1/3}[2y^{-1/2}] \tag{16a}$$

$$L^{-1}\{\exp[-3\varepsilon^{1/3}]\} = \frac{3^{1/2}}{\pi y^{3/2}}K_{1/3}[2y^{-1/2}] \tag{16b}$$

which are defined if the real part of ε is strictly positive. $K_{1/3}(y)$ is the Hankel function of the second kind and of parameter $\frac{1}{3}$. The quantity η_i is now expressed with its integer part, denoted by $E(\eta_i)$, and its decimal part $D(\eta_i)$

$$\eta_i = E(\eta_i) + D(\eta_i) \tag{17a}$$

If one refers to the definition of γ_i [Eq. (6)], then, one can remark that η_i does not depend on the coefficients ω_j, which are associated with the collisional model

$$\eta_i = \begin{cases}\zeta_t/2 + (\zeta_{1,i} + \zeta_{2,i})/2 + 1 & \text{if } i = 1\\ \zeta_t/2 + 1 & \text{if } i = 2\end{cases} \tag{17b}$$

The number of DOFs of the translational mode ζ_t is an integer. Moreover, for a continuous internal energy, the DOFs associated with the internal model $\zeta_{1,i}$ and $\zeta_{2,i}$ are also integers. As a consequence, the decimal part of η_i is either zero or equal to $\frac{1}{2}$. Thus, Eqs. (16a) and (16b) can write

$$L^{-1}\{\varepsilon^{-3D(\eta_i)}\exp[-3\varepsilon^{1/3}]\} = \frac{3^{1/2}}{\pi y^{3/2-2D(\eta_i)}}K_{1/3}[2y^{-1/2}] \tag{18}$$

Since the exponential is isolated to circumvent the difficulty, the inverse Laplace transform φ has to be replaced by the product of two functions Φ_1 and Φ_2

$$\Phi_1(\varepsilon_i) = \varepsilon_i^{-E(\eta_i)+2D(\eta_i)} \tag{19a}$$

$$\Phi_2(\varepsilon_i) = \varepsilon_i^{-3D(\eta_i)}\exp[-\beta\varepsilon_i^{1/3}] \tag{19b}$$

such as

$$\varphi(y_i) = L^{-1}[\Phi_1(\varepsilon_i)\cdot\Phi_2(\varepsilon_i)] \tag{19c}$$

The inverse Laplace transform of a product of two functions may be expressed with a convolution product.[17] First, the inverse Laplace transforms of Φ_1 and Φ_2 have to be determined. Next, their product of convolution is derived. The inverse Laplace transform of Φ_1 is immediately obtained[17]

$$\varphi_1(y_i) = L^{-1}[\Phi_1(\varepsilon_i)] = \frac{y_i^{E(\eta_i)-2D(\eta_i)-1}}{\Gamma[E(\eta_i) - 2D(\eta_i)]} \tag{20a}$$

since $E(\eta_i) - 2D(\eta_i)$ is strictly positive. On the other hand, to make use of the relation (18), in order to derive the inverse Laplace transform of Φ_2, the change of variable $\varepsilon_i^* = (\beta/3)^3\varepsilon_i$ is required. Then, the Laplace transformation properties, precised in Ref. 17, and Eq. (18) lead to

$$\varphi_2(y_i) = L^{-1}[\Phi_2(\varepsilon_i)] = (\beta/3)^{9D(\eta_i)-3} \times 3^{1/2}/\{\pi[(3/\beta)^3y_i]^{3/2-2D(\eta_i)}\}K_{1/3}[2(3/\beta)^{-3/2}y_i^{-1/2}] \tag{20b}$$

Finally, the integral relation is obtained as a convolution product[17] grouping together relations (19c), (20a), and (20b)

$$\varphi(y_i) = \left(\frac{\beta}{3}\right)^{3D(\eta_i)+3/2}\frac{3^{1/2}}{\pi\Gamma[E(\eta_i) - 2D(\eta_i)]} \times \int_0^{y_i}(y_i - x)^{E(\eta_i)-2D(\eta_i)-1}x^{-3/2+2D(\eta_i)} \times K_{1/3}\left[2\left(\frac{\beta}{3}\right)^{3/2}x^{-1/2}\right]dx \tag{21}$$

B. Step *S*2: Special Functions

First, one proceeds to the change of variable $x^* = 2(\beta/3)^{3/2}x^{-1/2}$ to simplify notations. Then, Eq. (21) writes

$$\Lambda^{-1}\varphi(y_i) = \int_{x_i^*}^{\infty}[(y_i^*)^2 - (x^*)^2]^{E(\eta_i)-2D(\eta_i)-1}(x^*)^{4D(\eta_i)}K_{1/3}[x^*]\,dx^* \tag{22}$$

where λ, y_i^*, and Λ are, respectively, defined in Eqs. (11d–11f). Since the decimal part of η_i is either 0 or equal to $\frac{1}{2}$ when the internal energy is supposed to be continuous, $E(\eta_i) - 2D(\eta_i) - 1$ is an integer. The first term appearing in the previous integral can then be developed and Eq. (22) writes

$$\Lambda^{-1}\varphi(y_i) = \sum_{j=0}^{2E(\eta_i)}{}^{2}a_j\int_{x_i^*}^{\infty}(x^*)^{-j}K_{1/3}[x^*]\,dx^* \tag{23a}$$

with

$$\sum_{j=0}^{2E(\eta_i)}{}^{2}a_j(x^*)^{-j} = [(y_i^*)^2 - (x^*)^2]^{E(\eta_i)-2D(\eta_i)-1}(x^*)^{4D(\eta_i)} \tag{23b}$$

The integral involved in Eq. (23a) is obtained performing integrations by parts and using the recurrence properties[18] of the Hankel function of the second kind. The result of the integration is given by the global expression

$$\int_{y_i}^{\infty} (x^*)^{-j} K_\nu[x^*]\,dx^* = \sum_{k=-j+1}^{j-1} b_k(\nu, y_i^*) K_{\nu+k}[y_i^*] + c(\nu, y_i^*) \int_{y_i}^{\infty} K_\nu[x^*]\,dx^*, \qquad \nu = \frac{1}{3} \tag{24}$$

where $b_k(\nu, y_i^*)$ and $c(\nu, y_i^*)$ are polynomial functions. We obtain the Airy function,[19] in the integral of the previous relation with a change of variable $x = \frac{2}{3}y^{3/2}$. Then, relation (24) is

$$\int_{y_i}^{\infty} (x^*)^{-j} K_\nu[x^*]\,dx^* = \sum_{k=-j+1}^{j-1} b_k(\nu, y_i^*) K_{\nu+k}[y_i^*] + \pi 3^{1/2} c(\nu, y_i^*) \int_{y_i^{**}}^{\infty} Ai(x)\,dx, \qquad \nu = \frac{1}{3} \tag{25}$$

where y_i^{**} is defined in Eq. (11g). Thus, φ expression may be written

$$\begin{aligned}\Lambda^{-1}\varphi[y_i] &= \sum_{j=0}^{2E(\eta_i)-2} a_j \left\{ \sum_{k=-j+1}^{j-1} b_k(\nu, y_i^*) K_{\nu+k}[y_i^*] \right\} + \pi 3^{1/2} c(\nu, y_i^*) \int_{y_i}^{\infty} Ai(x)\,dx \\ &= \sum_{k=-2E(\eta_i)+3}^{2E(\eta_i)-3} c_k(\nu, y_i^*) K_{\nu+k}[y_i^*] + \pi 3^{1/2} c(\nu, y_i^*) \int_{y_i^{**}}^{\infty} Ai(x)\,dx \end{aligned} \tag{26}$$

where $\nu = \frac{1}{3}$. The $\xi(y_i)$ function, stated Eq. (10b), is obtained by replacing $\varphi(y_i)$ in the relation (15a). The individual probability, stated in Eq. (10a), is then derived from Eq. (5a).

The asymptotic expansion of $\xi(y_i)$ function, we have proposed in Eq. (12), is derived from Eq. (10b) using asymptotic expansions of modified Bessel functions of second-order and Airy function integral when y tends to infinity. The former is given explicitly in Ref. 19 and the latter can be derived (see Ref. 16 for the details) from recurrence properties[19]

$$\int_y^{\infty} Ai(x)\,dx = \frac{1}{2\pi^{1/2}} y^{-1/4} \exp\left[-\frac{2}{3}y^{3/2}\right] \times \sum_{k=0}^{\infty} (-1)^k b_k \left(\frac{2}{3}y^{3/2}\right)^{-k} \tag{27a}$$

with

$$b_k = a_k + \left(k - \frac{1}{2}\right) b_{k-1} \tag{27b}$$

$$a_0 = 1 \quad \text{and} \quad a_k = \frac{\Gamma[3k + \frac{1}{2}]}{54^k k! \Gamma[k + \frac{1}{2}]} \tag{27c}$$

Its three first terms are also given in Ref. 20 (in the Appendix).

V. Numerical Applications: Results and Discussions

Individual probabilities curves associated with three DOFs in the velocity space are plotted in Figs. 1 and 2 when ϕ_i represents, respectively, the relative velocity norm and the total energy involved in the exchange. They have been calculated considering diatomic nitrogen and assuming $\Lambda_{ij} = 1$ and $jmax = 1$ to do consistent comparisons with models developed by Boyd[4] and Bird.[8] If one compares (Fig. 1), the individual probability approximated by Boyd thanks to the steepest decent method, curve $c1$, and the exact model derived with the Laplace transformation, curve $c2$, one can notice the great influence of the resolution method on p, especially for high velocities, as expected. In the same way Fig. 2 points out a great difference (several orders of magnitude) between Bird's empirical model, curve $c1$, and the exact one, curve $c2$, when energy is large. The gap in relation to macroscopic frequency of inelastic collisions to be reproduced is illustrated below considering an homogeneous test case. Before going further concerning the improvement of exact models on previous ones, the discussion is focused on computational aspects concerning the exact p.

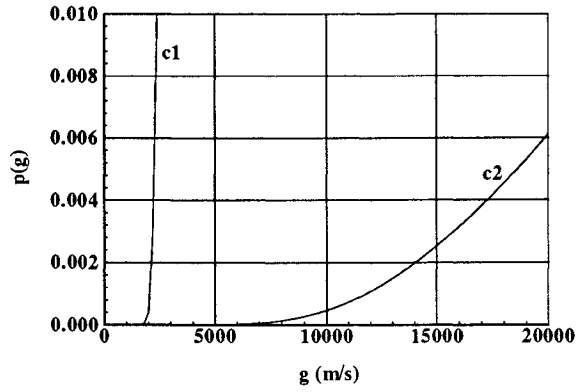

Fig. 1 Individual probabilities of vibration translation energy exchange associated with the relaxation time of Millikan and White, the chemical species N_2, the VHS collisional model, and expressed as a function of g. $c1$: model proposed by Boyd[4]; $c2$: exact model, Eq. (10a) with $jmax = 1$, $i = 2$, and $\zeta_t = 3$.

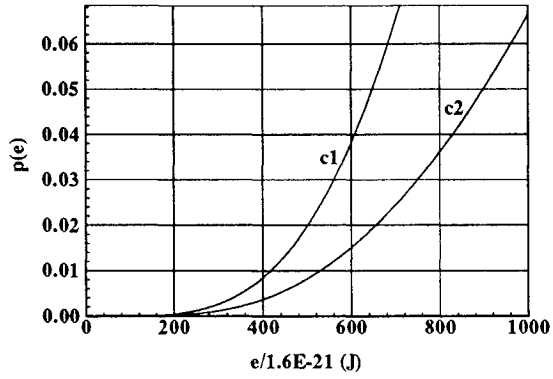

Fig. 2 Individual probabilities of vibration translation energy exchange associated with the relaxation time of Millikan and White, the chemical species N_2, the VHS collisional model, and expressed as a function of e. $c1$: model proposed by Bird[8]; $c2$: Eq. (10a) with $jmax = 1$, $i = 1$, and $\zeta_t = 3$.

The exact p expression, introduced in Sec. III, is more complex than models proposed by Boyd and Bird. These last ones involve a power term and an exponential function. The exact p, defined in Eq. (10a), includes a finite summation, polynomial functions, special functions K_ν and Ai, and an integral. As the exponential function, special functions are calculated using a mathematical library—NAG or MATLAB in the present case. The Airy function integral is calculated from zero to y_i^{**} with the Romberg method.[21] Its integral from zero to infinity is $\frac{1}{3}$. Since NAG tabulations of K_ν and Ai functions are available over the range]0; 9], beyond p is calculated using the asymptotic expansion proposed in Eq. (12). To minimize numerical operations, and thus time penalty applying numerically p model, we tabulate p expression.

Table 3 Gas characteristics

Molecular mass	4.640×10^{-26} kg
Numerical density	1.61×10^{21} mol/m^3
Reference temperature	273 K
Reference diameter	4.105×10^{-10} m
ω	0.24
κ	1.813×10^{-16} IS
A	220
B	−24.80

Table 4 Test case

Vibrational model	Figures
$p(g)$ model of Boyd, $\zeta_t = 3$	3a and 3b
$p(g)$ Eq. (10a), $jmax = 1$, $\zeta_t = 3$	4a and 4b
$p(e)$ model of Bird, $\zeta_t = 3$	5a and 5b
$p(e)$ Eq. (10a), $jmax = 1$, $\zeta_t = 3$	6a–6c

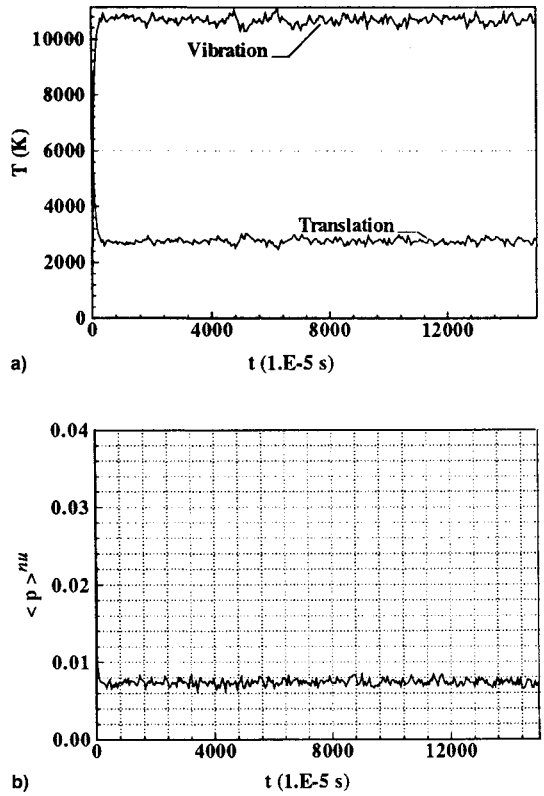

Fig. 3 Temporal evolution of a) temperatures and b) inelastic collision fractions; Boyd's model (Ref. 4).

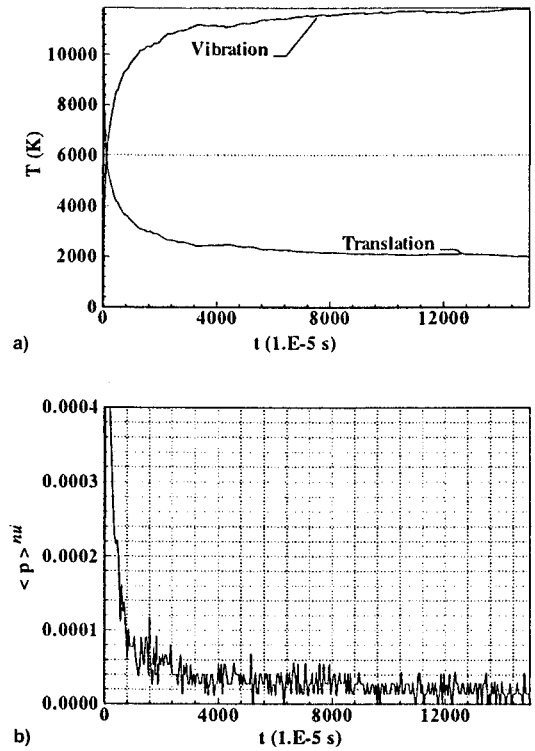

Fig. 4 Temporal evolution of a) temperatures and b) inelastic collision fractions; exact model, Eq. (10a) with $\phi_i = g$, $\zeta_t = 3$, $jmax = 1$.

The energy step used to determine $p(e)$ is $1.6 \times 10^{-21} J$; joining between exact p and its asymptotic expansion is made continuous using a fit program.[21] Parameters involved in Eqs. (10a) and (12) depend only on the chemical species under consideration. Consequently, we emphasize that p tabulation applies to any problem of rarefied flow with high enthalpy. With this one input table, computational cost is not increased in comparison with previous microscopic models.

Calculations using the DSMC method and the original BL scheme are realized to check that p models of Sec. III lead to a thermal equilibrium in good agreement with theory and, also, reproduce the theoretical fraction of inelastic collisions at equilibrium. In that aim, the homogeneous unsteady problem of a pure diatomic gas of nitrogen, initially presenting a nonequilibrium between vibrational and translational modes is studied considering 1000 simulated particles. Initial temperatures of vibration and translation are, respectively, set to 0 and 10,000 K. A smaller initial nonequilibrium, presented in Ref. 16, leads to similar results. Gas characteristics are given in Table 3. Collisional model coefficient ω is fitted to the viscosity law of Poiseuille. Investigated models are indicated in Table 4. Numerical results obtained at equilibrium (denoted by the superscript nu), and theoretical ones (denoted by the superscript th), are brought together in Table 5 to make the comparison easier.

Figures 3a and 4a clearly show that none of the p models expressed explicitly as a function of the relative velocity norm, and applied using the original BL scheme, reproduces the equipartition of energy at equilibrium. This goes with an overestimation of the theoretical fraction of inelastic collisions (cf. Figs. 3b and 4b). These negative results, which are much more flagrant than for rotational energy,[11,16] hold true for any resolution method, even exact. This comes from the violation of hypothesis $H5$. The total collision cross section of the GHS model [Eq. (2)] is homogeneous with respect to the relative velocity norm when $jmax$ is set to unity (cf. Ref. 11 for $jmax$ greater than one). Individual probability $p(g)$, given in Eq. (10a), and Boyd's model are not homogeneous with respect to g; thus, relation (1) is not satisfied and the entropy theorem associated with the original BL scheme is not verified. Therefore, these numerical results are in perfect agreement with the mathematical study carried out by Bourgat et al.,[12] and $p(g)$ models under consideration cannot be applied within the frame of the original BL scheme. However, one could consider new versions of this scheme proposed by Abe[22] considering the VHS cross section and by Hash et al.[14] concerning the GHS model.

Individual probabilities developed under assumption $H4a$, such as Bird's model and the exact model [Eq. (10a)], depend on a collisional invariant since they are functions of the total energy involved in the exchange. One can verify (Figs. 5a and 6a) that they reproduce detailed balance at equilibrium within the frame of the original BL scheme. In addition, this is confirmed by distribution functions of vibrational energy. Results presented in Ref. 8 and Fig. 6b concerning, respectively, the

Table 5 Numerical and theoretical results obtained at equilibrium

	Figures			
	3	4	5	6
T^{th}, K	6,000	6,000	6,000	6,000
T_{tr}^{mc}, K	2,800	2,200	6,000	6,000
T_{v}^{mc}, K	10,800	11,700	6,000	6,000
$\langle p \rangle^{th}$	9.3×10^{-6}	9.3×10^{-6}	9.3×10^{-6}	9.3×10^{-6}
$\langle p \rangle^{mc}$	$(7.5 \pm 0.5) \times 10^{-3}$	$(2 \pm 1) \times 10^{-5}$	$(1.5 \pm 0.1) \times 10^{-3}$	$(9.5 \pm 0.5) \times 10^{-6}$

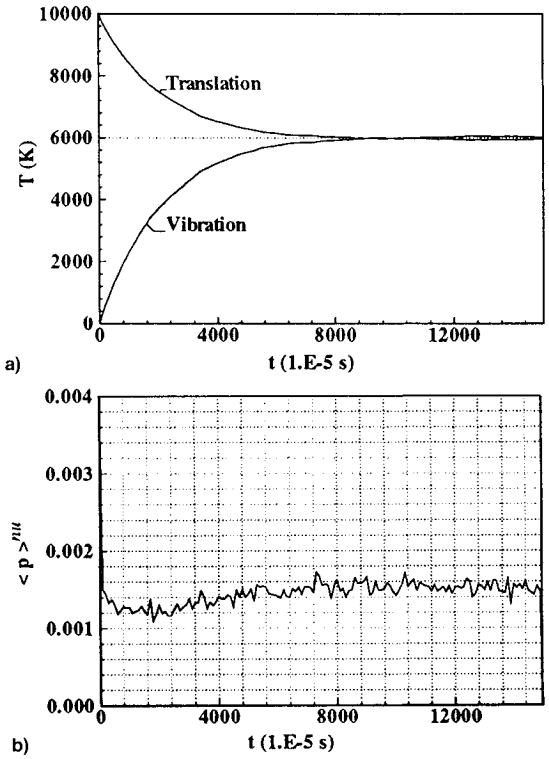

Fig. 5 Temporal evolution of a) temperatures and b) inelastic collision fractions; Bird's model (Ref. 8).

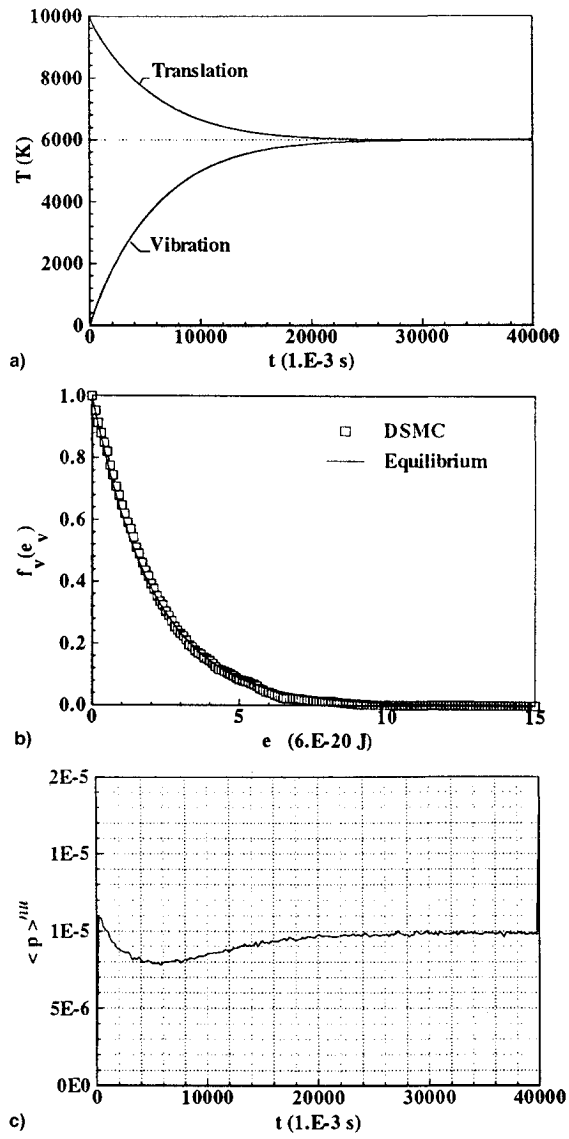

Fig. 6 a) Temporal evolution of temperatures; exact model, Eq. (10a) with $\phi_i = e/\Lambda_G$, $\zeta_t = 3$, $jmax = 1$, $\Lambda_G = 2.1364$. b) Distribution function for the vibrational energy. *c*1: numerical solution with exact model, $\phi_i = e/\Lambda_G$, $\zeta_t = 3$, $jmax = 1$, $\Lambda_G = 2.1364$; *c*2: equilibrium solution (Hinshelwood). c) Temporal evolution of inelastic collision fractions; exact model, Eq. (10a) with $\phi_i = e/\Lambda_G$, $\zeta_t = 3$, $jmax = 1$, $\Lambda_G = 2.1364$.

model proposed by Bird and the exact model, are in excellent agreement with the Boltzmann distribution. Indeed, the relation (1) and, thus, the entropy theorem, are now verified. However, the empirical model (Fig. 5b) overestimates the theoretical fraction of inelastic collisions by a factor of 160. Notice that, according to Fig. 2, this factor increases with temperature. When a rarefied flow with high enthalpy is simulated numerically, this discrepancy factor affects in proportion the time needed to reach detailed balance and, thus, temperature distributions, mainly in nonequilibrium areas. When Λ_G is set to unity, the exact model $p(e)$, with $e = \mu g^2/2 + e_v$, leads also to an underestimation of the time needed to reach equilibrium (by a factor 25 in the present case). As underlined by Haas,[23] this phenomenom is due to a biasing of the distribution function associated with the subset selected for energy exchange after collision. Calculations presented in Figs. 6a–6c are associated with the appropriate constant value for Λ_G defined in Eq. (7) ($\Lambda_G = 2.1364$ in the present case), and the exact model $p(e)$ [Eq. (10a)], with $e = (\mu g^2/2 + e_v)/\Lambda_G$. This exact model reproduces (Fig. 6c) the theoretical fraction of inelastic collisions with an excellent accuracy. Moreover, computational cost of calculations performed with Bird's model and the exact model differ from one another by less than 2%. The improvement obtained with an exact derivation of p is thus very beneficial, even for repulsive intermolecular potentials, all the more that tabulated exact p is as competitive in computational time as previous empirical or approximated models.

VI. Concluding Remarks

The class of models proposed here possesses several new features, improving previous models.[4,8] It is extended from repulsive to repulsive–attractive intermolecular potential thanks to the systematic and exact resolution method based on the Laplace transformation.[11] It reproduces, on average, Millikan and White's relaxation time over all its domain of validity. Former restriction to the characteristic temperature of vibrational excitation is now avoided. It includes previous models

developed by Boyd, and also Bird, as borderline cases. When expressed as a function of a collisional invariant, models introduced in this article fulfill detailed balance at equilibrium within the frame of the original BL scheme. This property is justified by the entropy theorem verification. Moreover, fraction of inelastic collisions, strongly overestimated by approximate or empirical models, is well-reproduced by the exact model. At last, although exact p expression could seem complex, it does not cause time penalty when tabulated.

Expressions obtained in this first approach, assuming a continuous vibrational energy, are also useful to determine individual probabilities associated with a discrete energy of vibration. These discrete models are presented in a forthcoming paper constituting the second part of the study.

Appendix: Coefficients C_j

We refer the reader to Ref. 16 for the details of the derivations.

Three Dimensions in the Velocity Space, $\zeta_r = 3$

Particular Case $i = 1$, $\zeta_{1,v} = 2$, $\zeta_{2,v} = 2$

In this particular case, $\gamma_1 = 4$, thus, $E(\eta_1) = 4$, $D(\eta_1) = \frac{1}{2}$, and

$$\xi(y_1) = \alpha\Lambda \left\{ \sum_{j=-5}^{5} c_j(\nu, y_1^*) K_{\nu+j}[y_1^*] + \pi 3^{1/2} c(\nu, y_1^*) \int_{y_1}^{\infty} Ai[x]\, dx \right\} \tag{A1}$$

$$c_{-5}(\nu, \lambda e^{-1/2}) = \frac{1}{3840(\nu - 5)} \tag{A2a}$$

$$c_{-4}(\nu, \lambda e^{-1/2}) = \frac{1}{1920} \lambda^{-1} e^{1/2} \tag{A2b}$$

$$c_{-3}(\nu, \lambda e^{-1/2}) = \frac{1}{24} \lambda^{-2} e \left[\frac{-1}{\nu - 3} - \frac{1}{40} \right] + \frac{1}{768} \left[\frac{1}{\nu - 3} - \frac{2}{5(\nu - 5)} \right] \tag{A2c}$$

$$c_{-2}(\nu, \lambda e^{-1/2}) = -\frac{19}{240} \lambda^{-3} e^{3/2} + \frac{1}{480} \lambda^{-1} e^{1/2} \tag{A2d}$$

$$c_{-1}(\nu, \lambda e^{-1/2}) = \frac{1}{2} \lambda^{-4} e^2 \left[\frac{1}{\nu - 1} + \frac{17}{60} \right] + \frac{1}{8} \lambda^{-2} e \left[\frac{-1}{\nu - 1} + \frac{2}{3(\nu - 3)} - \frac{1}{40} \right] + \frac{1}{384} \left[\frac{1}{\nu - 1} - \frac{1}{\nu - 3} + \frac{1}{5(\nu - 5)} \right] \tag{A2e}$$

$$c_0(\nu, \lambda e^{-1/2}) = \frac{8}{15} \lambda^{-5} e^{5/2} - \frac{19}{120} \lambda^{-3} e^{3/2} + \frac{1}{320} \lambda^{-1} e^{1/2} \tag{A2f}$$

$$c_1(\nu, \lambda e^{-1/2}) = \frac{1}{2} \lambda^{-4} e^2 \left[\frac{-1}{\nu + 1} + \frac{17}{60} \right] + \frac{1}{8} \lambda^{-2} e \left[\frac{1}{\nu + 1} - \frac{2}{3(\nu + 3)} - \frac{1}{40} \right] + \frac{1}{384} \left[\frac{-1}{\nu + 1} + \frac{1}{\nu + 3} - \frac{1}{5(\nu + 5)} \right] \tag{A2g}$$

$$c_2(\nu, \lambda e^{-1/2}) = c_{-2}(\nu, \lambda e^{-1/2}) \tag{A2h}$$

$$c_3(\nu, \lambda e^{-1/2}) = \frac{1}{24} \lambda^{-2} e \left[\frac{1}{\nu + 3} - \frac{1}{40} \right] + \frac{1}{768} \left[\frac{-1}{\nu + 3} + \frac{2}{5(\nu + 5)} \right] \tag{A2i}$$

$$c_4(\nu, \lambda e^{-1/2}) = c_{-4}(\nu, \lambda e^{-1/2}) \tag{A2j}$$

$$c_5(\nu, \lambda e^{-1/2}) = \frac{-1}{3840(\nu + 5)} \tag{A2k}$$

$$c(\nu, \lambda e^{-1/2}) = -\lambda^{-4} e^2 \frac{1}{\nu^2 - 1} + \frac{1}{4} \lambda^{-2} e \left[\frac{1}{\nu^2 - 1} - \frac{1}{\nu^2 - 9} \right] + \frac{1}{128} \left[\frac{-2}{3(\nu^2 - 1)} + \frac{1}{\nu^2 - 9} - \frac{1}{3(\nu^2 - 25)} \right] \tag{A2l}$$

Particular Case $i = 1$, $\zeta_{1,v} = 2$, $\zeta_{2,v} = 0$

In this particular case, $\gamma_1 = 3$, thus $E(\eta_1) = 3$, $D(\eta_1) = \frac{1}{2}$ and

$$\xi(y_1) = \alpha\Lambda \left\{ \sum_{j=-3}^{3} c_j(\nu, y_1^*) K_{\nu+j}[y_1^*] + \pi 3^{1/2} c(\nu, y_1^*) \int_{y_1}^{\infty} Ai[x]\, dx \right\} \tag{A3}$$

$$c_{-3}(\nu, \lambda e^{-1/2}) = \frac{-1}{48(\nu - 3)} \tag{A4a}$$

$$c_{-2}(\nu, \lambda e^{-1/2}) = \frac{1}{24} \lambda^{-1} e^{1/2} \tag{A4b}$$

$$c_{-1}(\nu, \lambda e^{-1/2}) = \frac{1}{2} \lambda^{-2} e \left[\frac{1}{\nu - 1} + \frac{1}{6} \right] + \frac{1}{16} \left[\frac{-1}{\nu - 1} + \frac{2}{3(\nu - 3)} \right] \tag{A4c}$$

$$c_0(\nu, \lambda e^{-1/2}) = \frac{2}{3} \lambda^{-3} e^{3/2} - \frac{1}{12} \lambda^{-1} e^{1/2} \tag{A4d}$$

$$c_1(\nu, \lambda e^{-1/2}) = \frac{1}{2} \lambda^{-2} e \left[\frac{-1}{\nu + 1} + \frac{1}{6} \right] + \frac{1}{16} \left[\frac{1}{\nu + 1} - \frac{2}{3(\nu + 3)} \right] \tag{A4e}$$

$$c_2(\nu, \lambda e^{-1/2}) = c_{-2}(\nu, \lambda e^{-1/2}) \tag{A4f}$$

$$c_3(\nu, \lambda e^{-1/2}) = \frac{1}{48(\nu + 3)} \tag{A4g}$$

$$c(\nu, \lambda e^{-1/2}) = -\lambda^{-2} e \frac{1}{\nu^2 - 1} + \frac{1}{8} \left[\frac{1}{\nu^2 - 1} - \frac{1}{\nu^2 - 9} \right] \tag{A4h}$$

Particular Case $i = 2$

In this particular case, $\gamma_2 = 2$, thus, $E(\eta_2) = 2$, $D(\eta_2) = \frac{1}{2}$, and

$$\xi(y_2) = \alpha\Lambda \left\{ \sum_{j=-1}^{1} c_j(\nu, y_2^*) K_{\nu+j}[y_2^*] + \pi 3^{1/2} c(\nu, y_2^*) \int_{y_2}^{\infty} Ai[x]\, dx \right\} \tag{A5}$$

$$c_{-1}(\nu, \lambda g^{-1}) = \frac{1}{2(\nu - 1)} \tag{A6a}$$

$$c_0(\nu, \lambda g^{-1}) = \lambda^{-1} g \tag{A6b}$$

$$c_1(\nu, \lambda g^{-1}) = \frac{-1}{2(\nu + 1)} \tag{A6c}$$

$$c(\nu, \lambda g^{-1}) = \frac{-1}{\nu^2 - 1} \tag{A6d}$$

Two Dimensions in the Velocity Space, $\zeta_i = 2$

Particular Case $i = 1$, $\zeta_{1,v} = 2$, $\zeta_{2,v} = 2$

For this particular case, $\gamma_1 = \frac{7}{2}$, thus, $E(\eta_1) = 4$, $D(\eta_1) = 0$, and

$$\xi(y_1) = \alpha\Lambda \left\{ \sum_{j=-5}^{5} c_j(\nu, y_1^*) K_{\nu+j}[y_1^*] + \pi 3^{1/2} c(\nu, y_1^*) \int_{y_1^*}^{\infty} Ai[x]\, dx \right\} \tag{A7}$$

$$c_{-5}(\nu, \lambda e^{-1/2}) = \frac{-1}{3840(\nu - 5)} \tag{A8a}$$

$$c_{-4}(\nu, \lambda e^{-1/2}) = \frac{-1}{1920} \lambda^{-1} e^{1/2} \tag{A8b}$$

$$c_{-3}(\nu, \lambda e^{-1/2}) = \frac{1}{16} \lambda^{-2} e \left[\frac{1}{\nu - 3} + \frac{1}{60} \right] + \frac{1}{768} \left[\frac{-1}{\nu - 3} + \frac{2}{5(\nu - 5)} \right] \tag{A8c}$$

$$c_{-2}(\nu, \lambda e^{-1/2}) = \frac{29}{240} \lambda^{-3} e^{3/2} - \frac{1}{480} \lambda^{-1} e^{1/2} \tag{A8d}$$

$$c_{-1}(\nu, \lambda e^{-1/2}) = \frac{3}{2} \lambda^{-4} e^2 \left[\frac{-1}{\nu - 1} - \frac{3}{20} \right] + \frac{3}{16} \lambda^{-2} e \left[\frac{1}{\nu - 1} - \frac{2}{3(\nu - 3)} + \frac{1}{60} \right] + \frac{1}{384} \left[\frac{-1}{\nu - 1} + \frac{1}{\nu - 3} - \frac{1}{5(\nu - 5)} \right] \tag{A8e}$$

$$c_0(\nu, \lambda e^{-1/2}) = -\frac{11}{5} \lambda^{-5} e^{5/2} + \frac{29}{120} \lambda^{-3} e^{3/2} - \frac{1}{320} \lambda^{-1} e^{1/2} \tag{A8f}$$

$$c_1(\nu, \lambda e^{-1/2}) = \frac{3}{2} \lambda^{-4} e^2 \left[\frac{1}{\nu + 1} - \frac{3}{20} \right] + \frac{3}{16} \lambda^{-2} e \left[\frac{-1}{\nu + 1} + \frac{2}{3(\nu + 3)} + \frac{1}{60} \right] + \frac{1}{384} \left[\frac{1}{\nu + 1} - \frac{1}{\nu + 3} + \frac{1}{5(\nu + 5)} \right] \tag{A8g}$$

$$c_2(\nu, \lambda e^{-1/2}) = c_{-2}(\nu, \lambda e^{-1/2}) \tag{A8h}$$

$$c_3(\nu, \lambda e^{-1/2}) = \frac{1}{16} \lambda^{-2} e \left[\frac{-1}{\nu + 3} + \frac{1}{60} \right] + \frac{1}{768} \left[\frac{1}{\nu + 3} - \frac{2}{5(\nu + 5)} \right] \tag{A8i}$$

$$c_4(\nu, \lambda e^{-1/2}) = c_{-4}(\nu, \lambda e^{-1/2}) \tag{A8j}$$

$$c_5(\nu, \lambda e^{-1/2}) = \frac{1}{3840(\nu + 5)} \tag{A8k}$$

$$c(\nu, \lambda e^{-1/2}) = \lambda^{-6} e^3 + \lambda^{-4} e^2 \frac{3}{\nu^2 - 1} + \frac{3}{8} \lambda^{-2} e \left[\frac{-1}{\nu^2 - 1} + \frac{1}{\nu^2 - 9} \right] + \frac{1}{128} \left[\frac{2}{3(\nu^2 - 1)} - \frac{1}{\nu^2 - 9} + \frac{1}{3(\nu^2 - 25)} \right] \tag{A8l}$$

Particular Case $i = 1$, $\zeta_{1,v} = 2$, $\zeta_{2,v} = 0$

In this particular case, $\gamma_1 = \frac{5}{2}$, thus, $E(\eta_1) = 3$, $D(\eta_1) = 0$, and

$$\xi(y_1) = \alpha\Lambda \left\{ \sum_{j=-3}^{3} c_j(\nu, y_1^*) K_{\nu+j}[y_1^*] + \pi 3^{1/2} c(\nu, y_1^*) \int_{y_1^*}^{\infty} Ai[x]\, dx \right\} \tag{A9}$$

$$c_{-3}(\nu, \lambda e^{-1/2}) = \frac{1}{48(\nu - 3)} \tag{A10a}$$

$$c_{-2}(\nu, \lambda e^{-1/2}) = \frac{1}{24} \lambda^{-1} e^{1/2} \tag{A10b}$$

$$c_{-1}(\nu, \lambda e^{-1/2}) = \lambda^{-2} e \left[\frac{-1}{\nu - 1} - \frac{1}{12} \right] + \frac{1}{8} \left[\frac{1}{2(\nu - 1)} - \frac{1}{3(\nu - 3)} \right] \tag{A10c}$$

$$c_0(\nu, \lambda e^{-1/2}) = -\frac{5}{3} \lambda^{-3} e^{3/2} + \frac{1}{12} \lambda^{-1} e^{1/2} \tag{A10d}$$

$$c_1(\nu, \lambda e^{-1/2}) = \lambda^{-2} e \left[\frac{1}{\nu + 1} - \frac{1}{12} \right] + \frac{1}{8} \left[\frac{-1}{2(\nu + 1)} + \frac{1}{3(\nu + 3)} \right] \tag{A10e}$$

$$c_2(\nu, \lambda e^{-1/2}) = c_{-2}(\nu, \lambda e^{-1/2}) \tag{A10f}$$

$$c_3(\nu, \lambda e^{-1/2}) = \frac{-1}{48(\nu + 3)} \tag{A10g}$$

$$c(\nu, \lambda e^{-1/2}) = \lambda^{-4} e^2 + \lambda^{-2} e \frac{2}{\nu^2 - 1} + \frac{1}{8} \left[\frac{-1}{\nu^2 - 1} + \frac{1}{\nu^2 - 9} \right] \tag{A10h}$$

Particular Case $i = 2$

In this particular case, $\gamma_2 = \frac{1}{2}$, thus, $E(\eta_2) = 1$, $D(\eta_2) = 0$, and

$$\xi(y_2) = \alpha\Lambda \left\{ \sum_{j=-1}^{1} c_j(\nu, y_1^*) K_{\nu+j}[y_1^*] + \pi 3^{1/2} c(\nu, y_1^*) \int_{y_1^*}^{\infty} Ai[x]\, dx \right\} \tag{A11}$$

$$c_{-1}(\nu, \lambda g^{-1}) = \frac{-1}{2(\nu - 1)} \tag{A12a}$$

$$c_0(\nu, \lambda g^{-1}) = -\lambda^{-1} g \tag{A12b}$$

$$c_1(\nu, \lambda g^{-1}) = \frac{1}{2(\nu + 1)} \tag{A12c}$$

$$c(\nu, \lambda g^{-1}) = \lambda^{-2} g^2 + \frac{1}{\nu^2 - 1} \tag{A12d}$$

Acknowledgments

The author wants to thank C. Marmignon for useful discussions during this work, J.-C. Lengrand for providing his numerical simulation code, and both for their comments on the manuscript. In addition the author has benefited from discussions with F. Coquel and L. Desvillettes. The author also acknowledges the constructive criticism of the reviewers, which have improved the quality of this article.

References

[1]Bird, G. A., *Molecular Gas Dynamics*, Clarendon, Oxford, England, UK, 1976.

[2]Borgnakke, C., and Larsen, P. S., "Statistical Collision Model for Monte Carlo Simulation of Polyatomic Gas Mixture," *Journal of Computational Physics*, Vol. 18, 1975, pp. 405–420.

[3]Millikan, R. C., and White, D. R., "Systematics of Vibrational Relaxation," *Journal of Chemical Physics*, Vol. 39, No. 12, 1963, pp. 3209–3213.

[4]Boyd, I. D., "Rotational and Vibrational Nonequilibrium Effects in Rarefied Hypersonic Flow," *Journal of Thermophysics and Heat Transfer*, Vol. 4, No. 4, 1990, pp. 478–484.

[5]Boyd, I. D., "Analysis of Vibrational-Translational Energy Transfer Using the Direct Simulation Monte Carlo Method," *Physics of Fluids A*, Vol. 3, No. 7, 1991, pp. 1785–1791.

[6]Bird, G. A., "Monte-Carlo Simulation in an Engineering Context," *Rarefied Gas Dynamics*, edited by S. S. Fisher, Vol. 74, Pt. I, Progress in Astronautics and Aeronautics, AIAA, New York, 1980, pp. 239–255.

[7]Boyd, I. D., "Analysis of Rotational Nonequilibrium in Standing Shock Waves of Nitrogen," *AIAA Journal*, Vol. 28, No. 11, 1990, pp. 1997–1999.

[8]Bird, G. A., "Molecular Gas Dynamics and Direct Simulation of Gas Flow," Clarendon, Oxford, England, UK, 1994.

[9]Koura, K., and Matsumoto, H., "Variable Soft Sphere Molecular Model for Inverse-Power-Law or Lennard-Jones Potential," *Physics of Fluids A*, Vol. 3, No. 10, 1991, pp. 2459–2465.

[10]Hash, D. B., and Hassan, H. A., "Monte Carlo Simulation Using Attractive-Repulsive Potentials," *Rarefied Gas Dynamics*, edited by B. D. Shizgal and D. P. Weaver, Vol. 159, Progress in Astronautics and Aeronautics, AIAA, Washington, DC, 1994, pp. 284–293.

[11]Choquet, I., "Thermal Nonequilibrium Modeling Using the Direct Simulation Monte Carlo Method: Application to Rotational Energy," *Physics of Fluids A*, Vol. 6, No. 12, 1994, pp. 4042–4053.

[12]Bourgat, J.-F., Desvillettes, L., Le Tallec, P., and Perthame, B., "Microreversible Collisions for Polyatomic Gases and Boltzmann's Theorem," *European Journal of Mechanics Section B Fluids* (to be published).

[13]Haas, B. L., Hash, D. B., Bird, G. A., Lumpkin, F. E., and Hassan, H. A., "Rates of Thermal Relaxation in Direct Simulation Monte Carlo Methods," *Physics of Fluids A*, Vol. 6, No. 6, 1994, pp. 2191–2201.

[14]Hash, D. B., Moss, J. N., and Hassan, H. A., "Direct Simulation of Diatomic Gases Using the Generalized Hard Sphere Model," *Journal of Thermophysics and Heat Transfer*, Vol. 8, No. 4, 1994, pp. 758–764.

[15]Landau, V. L., and Teller, E., "Zur Theory der Schalldispersion," *Physikalische Zeitschrift der Sowjetunion*, Vol. 10, 1936, pp. 34–43.

[16]Choquet, I., "Modélisation des déséquilibres thermiques dans les écoulements de gas raréfiés," Thèse de l'Univ. Pierre et Marie Curie, Paris, France, Oct. 1993.

[17]Hadlik, J., "La transformation de Laplace à plusieurs variables," edited by Masson et Cie., Paris, 1969.

[18]Lebedev, N. N., "Special Functions and Their Applications," Clarendon, Oxford, England, UK, 1972.

[19]Anon., "Handbook of Mathematical Functions, with Formulas, Graphs, and Mathematical Tables," edited by M. Abramowitz, and I. A. Stegun, Dover, New York, 1970.

[20]Drazin, P., and Reid, W., "Hydrodynamic Stability," Cambridge Univ. Press, 1981.

[21]Press, W. H., Flannery, B. P., Teukolsky, S. A., and Vetterling, W. T., "Numerical Recipes. The Art of Scientific Computing," Cambridge Univ. Press, 1986.

[22]Abe, T., "New Model of DSMC for Internal-Translational Energy Transfer in Non-Equilibrium Flow," *Rarefied Gas Dynamics*, edited by B. D. Shizgal and D. P. Weaver, Vol. 159, Progress in Astronautics and Aeronautics, AIAA, Washington, DC, 1994, pp. 103–112.

[23]Haas, B. L., "Thermochemistry Models Applicable to a Vectorized Particle Simulation," Ph.D. Dissertation, Dept. of Aeronautics and Astronautics, Stanford Univ., Stanford, CA, Dec. 1990.